Free-Standing Photonic Glasses Fabricated in a Centrifugal Field

*Mengdi Chen, Danja Fischli, Lukas Schertel, Geoffroy J. Aubry, Benedikt Häusele, Sebastian Polarz, Georg Maret, and Helmut Cölfen**

One efficient method to obtain disordered colloidal packing is to reduce the stability of colloidal particles by adding electrolytes to the colloidal dispersions. But the correct amount of additional electrolytes must be found empirically. Here, the effect of $CaCl_2$ on polystyrene colloidal dispersions is studied, and a link between the amount of $CaCl_2$ and the corresponding glassy colloidal structure is quantitatively built. A threshold concentration of $CaCl_2$ is found by dynamic light scattering. When exceeding this threshold, different nanoparticle oligomers are observed in the dispersions by analytical ultracentrifugation. The second objective is to achieve free-standing samples, which is required for many optical measurements. A universal method is established, using a centrifugal field to produce robust samples by polymerizing coassembled hydrophilic monomers to form a network, which traps the glassy colloidal structures. Photon time of flight measurements shows that the $CaCl_2$ concentration threshold should not be exceeded. Otherwise an optical shortcut may take place. Thus, the work provides a feasible universal route to prepare macroscopic free-standing photonic glasses from electrostatically stabilized nanoparticles, suitable for further optical investigation.

Colloidal systems or colloidal dispersions are ubiquitous in both the natural environment and industrial processes. In the framework of nanofabrication by bottom-up synthetic chemistry, nanoparticle self-assembly is at the center of interest, due to the design possibilities of many functional constructs tailored toward a specific purpose.[1] One of the important uses of such colloidal systems is in photonic applications when the colloidal solid has a size in the order of the light wavelength.[2]

When the solid phase is built up of uniform spherical nanoparticles, for example polymeric latex spheres, regular and periodic arrays known as colloidal crystals are formed under proper conditions. Macroporous materials which are exact inverse replicas of colloidal crystals have been intensively investigated over the past two decades and play an important role in photonic crystal design.[3]

While photonic crystals take advantage of the periodicity in the dielectric constant to provide Bragg scattering of ballistic photons and photonic band gaps, random photonic media known as photonic glasses can also strongly affect light transport and exhibit interesting physical phenomena like random lasing[5] and possibly light localization.[4] However, contrary to intuition, to obtain high degrees of disorder from monodisperse building blocks is not an easy task. Methods like rapid sedimentation or modified vertical deposition have proven to be unsuccessful.[5] Therefore, most experimental

Dr. M. Chen, D. Fischli, B. Häusele, Prof. S. Polarz, Prof. H. Cölfen
Department of Chemistry
University of Konstanz
Universitätsstr. 10, 78457 Konstanz, Germany
E-mail: helmut.coelfen@uni-konstanz.de
L. Schertel, Dr. G. J. Aubry, Prof. G. Maret
Department of Physics
University of Konstanz
Universitätsstr. 10, 78457 Konstanz, Germany
L. Schertel
Department of Physics
University of Zurich
Winterthurerstr. 190, 8057 Zurich, Switzerland

DOI: 10.1002/smll.201701392

work on such random media has been based on materials, which are formed by particles with very broad size or shape distribution[6] and the individual electromagnetic response of each building block gives rise to an averaged-out optical response.[7] Resonant behavior of the scattering strength in monodisperse random media was reported[8] by which a new scattering regime might be reached in higher refractive index materials. García et al.[9] have done pioneering work and developed two promising routes to fabricate random materials from monodisperse colloidal particles, either by selectively etching one of the two kinds of spheres in a binary colloidal crystal or by introducing electrolyte to the monodisperse latex sphere dispersion to promote colloidal aggregation.

However, detailed knowledge about controlled ways to prepare randomly organized materials is still missing. Although the coagulation route is easy to handle and the coagulation of a charged colloidal dispersion has always been a core aspect of colloidal science,[10] there is a lack of understanding to precisely correlate the amount of electrolyte and the corresponding glassy colloidal packing. In addition, a reliable method to trigger the formation of the glassy colloidal packing as well as to preserve the structure at a macroscopic scale is still a significant challenge and in great demand.

Figure 1 shows the colloidal packing obtained from drying an aqueous monodisperse polystyrene colloidal dispersion under gravity. It can be easily found that the degree of disorder in the colloidal packing increases as the amount of $CaCl_2$ increases. When there is no salt present in the polystyrene dispersion, an ordered *fcc* arrangement was observed, as illustrated in Figure 1a. In the presence of electrolyte, the stability of a colloidal dispersion in which the colloidal particles are electrically charged decreases due to the charge screening by the electrolyte. The degree of order is getting lower and thus more voids are introduced when the concentration of $CaCl_2$ increased from 5.3×10^{-3} M (Figure 1b) to 10.7×10^{-3} M (Figure 1c).

Zeta (ξ) potential measurement is a conventional method to characterize the electrostatic stability of colloidal dispersions. When the magnitude of the zeta potential is small, attractive forces may exceed the electric repulsion between adjacent particles and the particles may aggregate and flocculate. Zeta potential measurements of the polystyrene colloidal dispersions at different concentrations of $CaCl_2$ are shown in Figure S1 (Supporting Information). It can be seen that up to a concentration of $CaCl_2$ of 10.7×10^{-3} M, the zeta potential remains smaller than –40 mV which indicates that the colloidal dispersions have good stability.[11] However, this does not correlate very well with what is observed in Figure 1 as the colloidal packing already started to lose its order at much lower electrolyte concentration.

Besides the Zeta potential measurements, there are several well-established methods to determine the stability of nanoparticles that can also be assessed via the size of the nanoparticle aggregates and to provide information concerning their surface modification. Dynamic light scattering (DLS) is one of the most widespread methods for sizing nanoparticles. We adopted it here trying to correlate the electrolyte concentration and the colloidal aggregate size. The results from

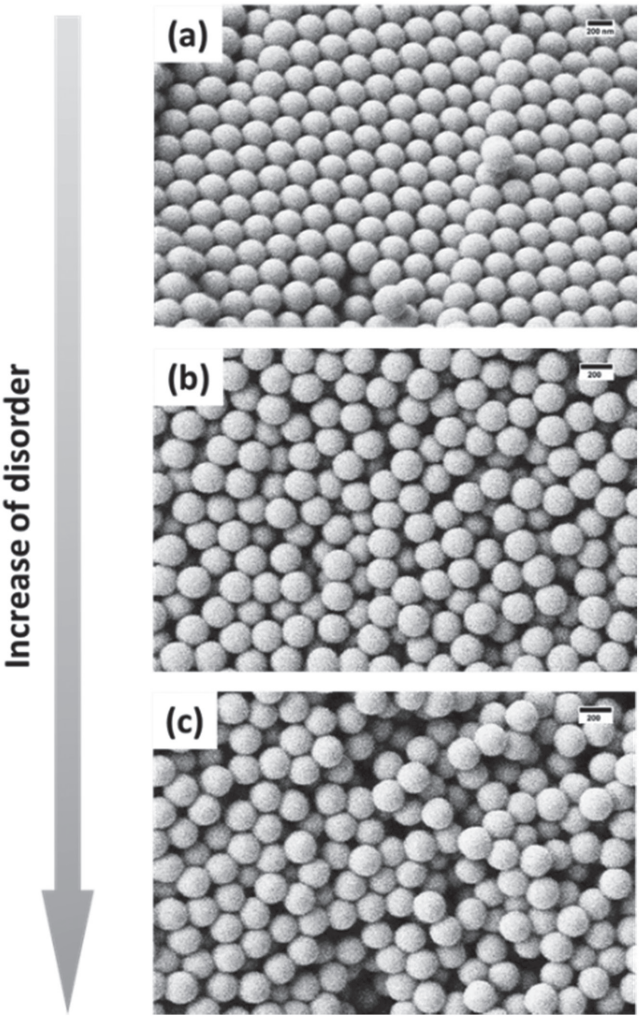

Figure 1. SEM images of colloidal packing obtained by drying a colloidal dispersion with different electrolyte concentration a) no $CaCl_2$, b) 5.3×10^{-3} M $CaCl_2$, and c) 10.7×10^{-3} M $CaCl_2$ under gravity. Scale bar = 200 nm.

DLS measurements are shown in **Figure 2**a. There is a small fluctuation in the particle sizes when small amounts of $CaCl_2$ are present. The average size increases at 10.7×10^{-3} M indicating aggregation although Figure 1 shows disorder already at lower electrolyte concentrations. Size distributions from DLS alone are nontrivial to obtain without prior knowledge of whether aggregation is occurring.[12]

In contrast, analytical ultracentrifugation (AUC) is very well suited to detect low levels of aggregation, since it combines extremely high resolution, up to Angstrom resolved particle size distributions,[13] with high statistical accuracy because every particle is detected. In Figure 2b, the $g^*(s)$ analysis has been used to calculate the sedimentation coefficient distribution.[14] Besides the primary peak, distinct peaks were found while the $CaCl_2$ concentrations were increased. These distinct peaks might presumably belong to different oligomers of the colloidal particles.

It is relatively straightforward to convert a sedimentation coefficient distribution into a particle size distribution assuming hard spheres using Equation (1):

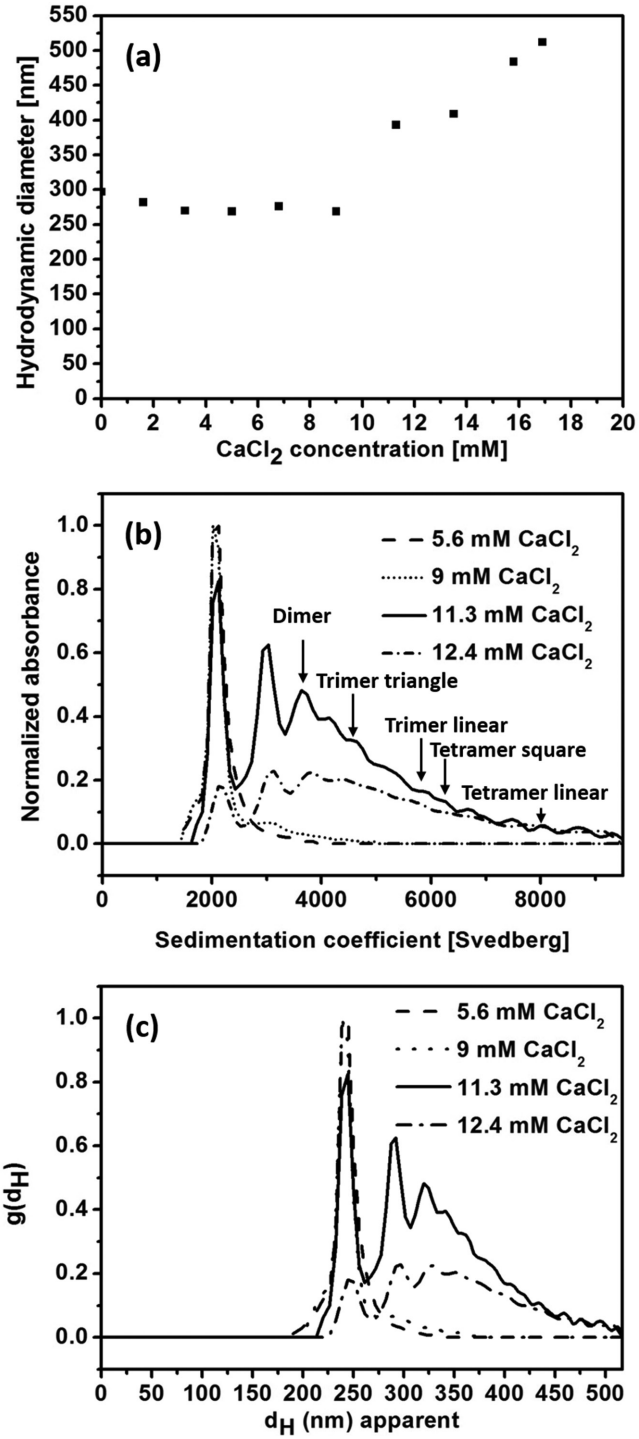

Figure 2. Determination of polystyrene particle sizes to detect the nanoparticle aggregation. a) The hydrodynamic diameter of the polystyrene colloidal particles measured by dynamic light scattering (DLS) at different electrolyte concentrations. b) The sedimentation coefficient distribution of the polystyrene colloidal particles measured by analytical ultracentrifugation (AUC) with different electrolyte concentrations. c) Particle size distribution converted from the sedimentation coefficient distribution.

$$d_p = \sqrt{\frac{18\eta_s s}{(\rho_P - \rho_s)}} \quad (1)$$

where d_p is the diameter of the particle, η_s is the viscosity of the medium, s is the sedimentation coefficient, ρ_s is the density of solvent and ρ_p is the density of the particle (1.054 g mL^{-1}). By calculating the sedimentation coefficients of the oligomeric structures[15] from the sedimentation coefficient of the monomer (2088 Svedberg), the values shown in **Table 1** are obtained. In Figure 2b, when the $CaCl_2$ concentration is 9×10^{-3} M, one species with the sedimentation coefficient of 3030 Svedberg showed up. But this species cannot be assigned to any of the oligomers in Table 1. When the concentration of $CaCl_2$ was increased to 11.3×10^{-3} M (Figure 2b), the species at 3030 Svedberg is more pronounced and a lot more distinct peaks including dimer, trimer triangle, trimer linear, tetramer square, and tetramer linear were observed. When the concentration of $CaCl_2$ went even higher to 12.4×10^{-3} M, the primary peak was weakened while the other oligomer species cannot be very well distinguished anymore. For easier comparison with other results, the sedimentation coefficients in Figure 2b and Table 1 were also converted to particle size (Figure 2c) via Equation (1). By combining the DLS and AUC analysis, it can be deduced that the polystyrene colloidal system experienced a transformation to a broad aggregate distribution when the concentration of $CaCl_2$ exceeded a certain threshold around 11×10^{-3} M.

Asymmetrical-flow-field-flow fractionation (AF4) investigations (Figure S2, Supporting Information) of the sample at 11.3×10^{-3} M Ca^{2+}, which only depends on the particle size, unlike size and density in AUC, did not show any species between monomer (250 nm) and dimer/trimer (350 nm). This means that the 3030 Svedberg species observed in AUC must be a monomer species with a higher density or a dimer with a lower density. Since the latexes are charge stabilized with sulfonate surface groups, binding of Ca^{2+} will occur, which not only leads to the observed oligomerization but also to a density increase. This is the likely explanation for the 3030 Svedberg species. Since it is relatively defined, we suspect that this species results from charge reversal by complete Ca^{2+} binding. Its higher density of 1.081 g mL^{-1} calculated from the size of 250 nm and s = 3030 Svedberg using Equation (1) supports this view as well as the fact that this species only becomes visible at higher Ca^{2+} concentrations starting at 9×10^{-3} M.

In order to approach a macroscopic material with glassy nanostructure, which could be suitable for further optical investigation (e.g., characterization of its resonant optical behavior),[8] a centrifugal force[3] which is easy and efficient to trigger colloidal assembly was applied here. The sediment at the bottom of the centrifuge tube was dried and investigated via scanning electron microscope (SEM). One can easily see from **Figure 3**a that the colloidal packing exhibits a two-layer structure when the amount of $CaCl_2$ is relatively far below the threshold (about 11×10^{-3} M obtained from DLS measurement shown in Figure 2a). At the top part, there were still some crystalline domains present while a random structure was observed at the bottom. This two-layer structure could be better recognized at lower magnification (see Figure S3, Supporting Information). Reflecting the AUC analysis in Figure 2b, at the chosen Ca^{2+} concentration of 5.3×10^{-3} M, the observed structure was built up by monomer nanoparticles, which however already have a tendency to aggregate. This becomes especially evident at the higher

Table 1. Sedimentation coefficient and hydrodynamic diameter of different polystyrene particle oligomers calculated from the sedimentation coefficient of the monomer.[15]

	Dimer	Trimer (triangle)	Trimer (linear)	Tetramer (square)	Tetramer (tetrahedron)	Tetramer (linear)
Sedimentation coefficient [Svedberg]	3712	4793	5800	6207	5611	8028
Hydrodynamic diameter [nm]	323	367	404	418	397	475

particle concentrations near the bottom of the centrifuge tube, where the particles are forced into the primary minimum in the DLVO (named after Boris Derjaguin, Lev Landau, Evert Verwey and Theodoor Overbeek) curve before they are able to form an ordered structure, which they would do in absence of salt. Nevertheless, at the lower particle concentrations at the top of the tube, ordered domains can still be formed (see Figure 3a).

If the amount of $CaCl_2$ is slightly increased, the dense monomer nanoparticles (3030 Svedberg) are formed. Thus, more domains with glassy structure were observed in Figure S4 (Supporting Information). The SEM images of colloidal packing prepared at 7.2×10^{-3} and 10.1×10^{-3} M $CaCl_2$ confirm this transition. It was found that the glassy domains occupied most of the sample at 7.2×10^{-3} M $CaCl_2$ while still some tiny crystalline parts can be found at the top of the sample. But when the concentration of $CaCl_2$ was increased to 10.1×10^{-3} M, crystalline domains become very sparse (Figure S4, Supporting Information).

Furthermore, when the amount of $CaCl_2$ exceeded the threshold, not only the two-layer structure disappeared but the whole structure shown in Figure 3b exhibited a random packing with many empty voids. This is caused by the different oligomers formed in presence of high $CaCl_2$ concentration. Therefore, it can be concluded that a random closed packed colloidal packing could be achieved by adding $CaCl_2$ to a concentration near but not exceeding the threshold concentration. The volume fractions of these close packed glasses were estimated to be <0.55.

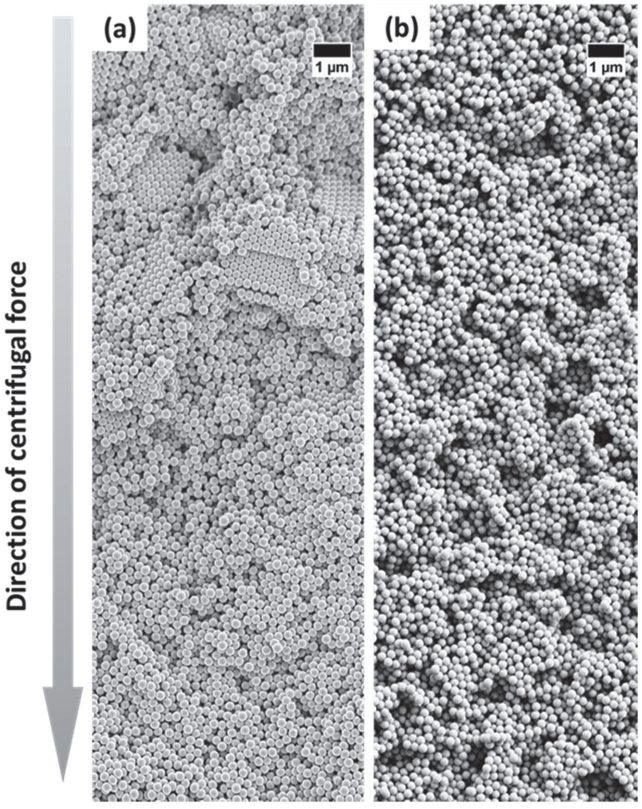

Figure 3. SEM images of colloidal glassy nanostructure prepared in a centrifugal field in presence of a) 5.3×10^{-3} M and b) 13.2×10^{-3} M $CaCl_2$.

Exceeding the threshold leads to holes (see Figure 3b) and thus to lower filling fraction. This might affect the light transport (weaker scattering) and lead to almost empty regions (holes) in the macroscopic sample where the light can propagate ballistically. The quality of the macroscopic samples can be characterized in photon time of flight experiments. A very short laser pulse (250 fs) is sent onto the sample and a time resolved photodetector measures in transmission for how long the photons traveled through the sample. If no holes are present, the photon transport through the sample follows a diffusion law. The time of flight distribution of a purely diffusive sample is known theoretically and fits the experiments very well.[6d] If holes are present in the sample, the photons entering these holes are much faster (they are not scattered until they exit the hole) and the overall transport through the sample is affected: the time of flight distribution does not follow a diffusion law anymore, since some photons leave the sample earlier than expected. This is why holes in such samples are called optical shortcuts. To perform such measurements as well as to carry out all other optical measurements, free-standing materials with a proper size (1 mm to 1 cm) are highly sought after. However, the colloidal assembly structures are in general quite fragile.

In order to preserve the very fragile colloidal assembly structures, we introduced here a coassembly method.[16] A hydrophilic monomer, in the present case acrylamide, was added into the colloidal dispersion. The coassembled structures were polymerized after centrifugation by addition of ammonia persulfate as initiator. Thus, the polystyrene colloidal spheres were trapped in the hydrogel. The robust hydrogel (see Figure S5, Supporting Information) can be easily taken out of the centrifuge tube and cut into the desired shape. Images of the monolithic samples can be found in Figure S6a (Supporting Information). The samples are centimeter scale, therefore big enough to preform optical measurements. Figure S6b,c (Supporting Information) shows the effect of the amount of polyacrylamide in between the polystyrene spheres. High concentration $CaCl_2$ caused the formation of different oligomers and created big volume fractions of voids (Figure S6c, Supporting Information). Therefore, more acrylamide monomers accumulated in between the polystyrene spheres and formed a thicker network after the polymerization.

This influences the light transport behavior of such samples. Light is scattered by interfaces between materials having

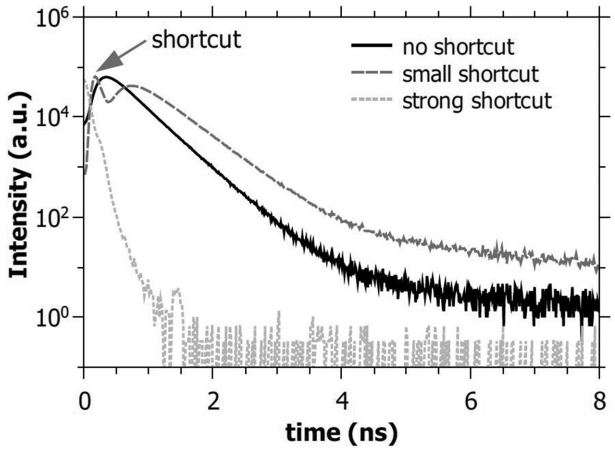

Figure 4. Photon time of flight measurements[6d] distinguishing samples with some big optical shortcuts (small dash curve: the photons leave the sample very early), some smaller optical shortcuts (small early peak in the dash curve indicated by an arrow), and without any optical shortcut (solid curve: all the photons behave diffusively).

different refractive indexes. High amounts of monomers and thus dense networks "connect" the particles optically and lower the scattering strength. In **Figure 4**, the photon time of flight distribution in a purely diffusive sample (e.g., the one of Figure S6b, Supporting Information) is shown in the solid curve. It can be easily distinguished from the sample of Figure S6c (Supporting Information), which has optical shortcuts (first peak from left side of the dash curve) corresponding to large voids in the spheres packing in which light travels without being scattered and therefore exits the sample earlier than in the diffusive sample. The small dash curve shows the time of flight of photons through a sample with at least one big optical shortcut (for example a crack in the sample): almost all photons went through and exited the sample very fast. We can make a hard cutoff to distinguish bad from good samples: Either a shortcut is visible or not.

In this work, we studied the influence of adding $CaCl_2$ to charge stabilized polystyrene colloidal systems via conventional methods like zeta potential measurement, which could not provide a satisfactory correlation with the observed colloidal packing. Alternatively, we incorporated dynamic light scattering, analytical ultracentrifugation, and asymmetrical flow field flow fractionation to characterize the colloidal particle size (distribution) in the presence of different amounts of $CaCl_2$ and successfully correlated the colloidal systems stability and the formation of different particle oligomers to the corresponding macroscopic colloidal packing structures. From the analytical ultracentrifugation analysis, a defined species, which was heavier than monomer particles appeared and became pronounced when the concentration of $CaCl_2$ increased to a certain threshold, which can be obtained by dynamic light scattering. When the amount of $CaCl_2$ was above this threshold, different oligomers of single polystyrene colloidal spheres were formed.

Furthermore, random colloidal packing was triggered by centrifugal force and was very well preserved on a macroscopic scale by trapping the random structure in a hydrogel. Photon time of flight measurements allowed us to characterize the macroscopic optical homogeneity of the samples prepared with different amounts of $CaCl_2$. To realize good sample quality, the amount of $CaCl_2$ should be limited to the threshold to avoid the formation of the oligomers which trigger optical shortcuts.

The fabrication route developed and the applied analytical methodology is universal for all charge stabilized nanoparticles since analytical ultracentrifugation is a high-resolution method for the characterization of particle size distributions[13] and can characterize all kinds of formed oligomers and particle clusters. Therefore, our methodology provides a promising materials basis for further optical investigations. This may be relevant not only for experimental studies of fundamental issues in light transport through random media (see, e.g., refs. [2,9], and [11]) but also for novel photonic applications such as diffuse reflectance standards.

Supporting Information

Supporting Information is available from the Wiley Online Library or from the author.

Acknowledgements

M.C. is funded by a Chinese Scholarship Council stipend. L.S., G.J.A., G.M., and H.C. acknowledge support from the Center for Applied Photonics (Universität Konstanz). G.J.A. acknowledges support from the Zukunftkolleg (Universität Konstanz) for an Independent Research Start-up Grant.

Conflict of Interest

The authors declare no conflict of interest.

[1] G. A. Ozin, K. Hou, B. V. Lotsch, L. Cademartiri, D. P. Puzzo, F. Scotognella, A. Ghadimi, J. Thomson, *Mater. Today* **2009**, *12*, 12.
[2] a) J. Ballato, *J. Opt. Soc. Am. B* **2000**, *17*, 219; b) S.-H. Kim, S. Y. Lee, S.-M. Yang, G.-R. Yi, *NPG Asia Mater.* **2011**, *3*, 25; c) D. S. Wiersma, *Nat. Photonics* **2013**, *7*, 188.
[3] G. von Freymann, V. Kitaev, B. V. Lotsch, G. A. Ozin, *Chem. Soc. Rev.* **2013**, *42*, 2528.
[4] P. W. Anderson, *Philos. Mag. B* **1985**, *52*, 505.
[5] P. D. García, R. Sapienza, C. López, *Adv. Mater.* **2010**, *22*, 12.
[6] a) N. M. Lawandy, R. Balachandran, A. Gomes, E. Sauvain, *Nature* **1994**, *368*, 436; b) L. F. Rojas-Ochoa, J. Mendez-Alcaraz, J. Sáenz, P. Schurtenberger, F. Scheffold, *Phys. Rev. Lett.* **2004**, *93*, 073903; c) M. Reufer, L. F. Rojas-Ochoa, S. Eiden, J. J. Sáenz, F. Scheffold, *Appl. Phys. Lett.* **2007**, *91*, 171904; d) T. Sperling, L. Schertel, M. Ackermann, G. J. Aubry, C. M. Aegerter, G. Maret, *New J. Chem. Phys.* **2016**, *18*, 013039.
[7] J. F. Galisteo-López, M. Ibisate, R. Sapienza, L. S. Froufe-Pérez, Á. Blanco, C. López, *Adv. Mater.* **2011**, *23*, 30.
[8] P. Garcia, R. Sapienza, J. Bertolotti, M. Martin, A. Blanco, A. Altube, L. Vina, D. Wiersma, C. López, *Phys. Rev. A* **2008**, *78*, 023823.

[9] P. D. García, R. Sapienza, Á. Blanco, C. López, *Adv. Mater.* **2007**, *19*, 2597.
[10] S. Xu, Z. Sun, *Soft Matter* **2011**, *7*, 11298.
[11] I. Ostolska, M. Wiśniewska, *Colloid Polym. Sci.* **2014**, *292*, 2453.
[12] J. B. Falabella, T. J. Cho, D. C. Ripple, V. A. Hackley, M. J. Tarlov, *Langmuir* **2010**, *26*, 12740.
[13] E. Karabudak, E. Brookes, V. Lesnyak, N. Gaponik, A. Eychmüller, J. Walter, D. Segets, W. Peukert, W. Wohlleben, B. Demeler, *Angew. Chem., Int. Ed.* **2016**, *55*, 11770.
[14] J. Lebowitz, M. S. Lewis, P. Schuck, *Protein Sci.* **2002**, *11*, 2067.
[15] A. J. Rowe, S. E. Harding, *Dynamic Properties of Biomolecular Assemblies*, Royal Society of Chemistry, Cambridge, UK, **1988**.
[16] J. H. Holtz, S. A. Asher, *Nature* **1997**, *389*, 829.

Received: May 1, 2017
Revised: June 11, 2017
Published online: July 19, 2017

